NMR AND AM1 QUANTUM CHEMICAL STUDY OF THE REGIOSELECTIVITY OF THE REACTION OF 2-HYDROXYETHYL METHACRYLATE WITH 3-NITROPHTHALIC ANHYDRIDE

Jaroslav KRIZ[1], Jiri DYBAL[2] and Zdenka SEDLAKOVA

Institute of Macromolecular Chemistry, Academy of Sciences of the Czech Republic, 162 06 Prague 6, Czech Republic; e-mail: [1] kriz@imc.cas.cz, [2] dybal@imc.cas.cz

Received September 5, 1996
Accepted October 18, 1996

The reaction of 2-hydroxyethyl methacrylate with 3-nitrophthalic anhydride catalyzed with triethylamine results in the 3 : 1 mixture of two possible monoesters, the more populated one being that with the ester group in ortho position to the nitro group. The isomers were identified and quantified by ^{1}H and ^{13}C 1D and 2D techniques including APT, INEPT, superselective long-range (SSLR) INEPT, SSLR HHCR, COSY, NOESY, HETCOR and COLOC. Theoretical analysis was done on the model reaction of methanol with the anhydride using semiempirical AM1 quantum chemical calculations. The results indicate that the relative regioselectivity of the reaction is due to both the electron distribution in the anhydride molecule and hydrogen bonding in the stages immediately preceding the transition state.

Key words: Regioselectivity of esterification; NMR; Quantum chemistry.

Aqueous solutions of polymers based on monoesters of 2-hydroxyethyl methacrylate (**1**) with substituted aromatic or pseudoaromatic anhydrides have a complex pH-dependent rheological behaviour offering promissing medical, e.g. ophthalmological application. For fyziological use, however, even slight differences in the structure of the ionogenic groups can be important. Thus the regioselectivity of the esterification of **1** with the incident substituted anhydride has to be determined but also predicted and theoretically explained. Partial esterification of a dicarboxylic acid anhydride with an alcohol is one of the oldest reactions in organic chemistry and can be considered trivial even in the case of less common anhydrides and alcohols. Less trivial, however, is both the determination and theoretical explanation or prediction of regioselectivity of such reaction if the anhydride in question is asymmetric. In the reaction of 2-hydroxyethyl methacrylate (**1**) or another alcohol with 3-nitrophthalic anhydride (**2**), two different regioisomers of the product, i.e. that with the ester group in the ortho position to the nitro group (**3**) and the other one with the same in meta position (**4**) can be formed. The well-known regioselectivity rules explaining most, e.g., electrophilic substitutions on the aromatic ring cannot be successfully used in this case because the electron distribution differences between carbonyl carbons in the anhydride group are rather small and

additional factors interfere. Also the expected steric effects of a large substituent, such as the *o*-nitro group in our case, do not control the regioselectivity as we show in this paper.

The second aim of this paper is thus to examine the ability of semiempirical quantum chemical methods of sufficient precision such as AM1 to predict and explain the course of the reaction. We treat this problem using methanol instead of **1** as the reaction partner of **2** because we want to discern the regiodirective interactions between the reactants along the reaction coordinate in a bare form. Complicating effects of the conformations of the far-away methacrylate part on the energy hypersurface of the reacting system probably would not add anything significant to its description.

EXPERIMENTAL

2-(2-Carboxy-6-nitrobenzoyloxy)ethyl Methacrylate (**3**) and 2-(2-Carboxy-3-nitrobenzoyloxy)ethyl Methacrylate (**4**)

To a mixture containing **2** (19.3 g, 0.1 mol), **1** (14.3 g, 0.11 mol) and 0.01 wt.% 1,1-diphenyl-2-picrylhydrazyl in benzene (25 ml) triethylamine (1.1 ml, 8 mmol) was added with stirring. After 3 h, the reaction was terminated by extraction of the reaction with 10% HCl thus removing the excess of **1** and the catalyst; the benzene layer containing **3** and **4** was extracted with 5% aqueous $NaHCO_3$ (250 ml) and the aqueous layer was repeatedly extracted with benzene. The aqueous layer was acidified to pH 2, and the product was extracted with benzene. After drying with Na_2SO_4 and distilling off the solvent at 2.1 kPa, the isolated product was freed of volatiles at 13.3 Pa and 25 °C. By precipitation of the product from $CHCl_3$ solution with heptane, the yellowish crystals were obtained in 89% yield. For $C_{14}H_{13}NO_8$ calculated: 51.97% C, 4.05% H, 4.33% N; found: 51.97% C, 4.03% H, 4.34% N.

NMR Measurements

NMR spectra (300.1 MHz for ^1H and 75.5 MHz for ^{13}C) were measured with a Bruker ACF 300 spectrometer at 297 K in deuteriochloroform with hexamethyldisiloxane as an internal standard which is 0.05 and 2 ppm shifted to TMS in ^1H and ^{13}C NMR, respectively. ^1H COSY (ref.[1]), NOESY (ref.[2]) and ROESY (ref.[3]) spectra were measured with 1 024 points and 512 increments, using the sinebell weighting function and symmetrization. The mixing time in NOESY was varied from 0.5 to 1.2 s. ^1H-^{13}C HETCOR (ref.[4]) and COLOC (ref.[5]) spectra were measured with 4 096 points and 256 increments with zero filling to 512 points in d1 dimension. The number of scans was 320 (HETCOR) and 1 024 (COLOC). Superselective long-range (SSLR) INEPT (ref.[6]) and SSLR HCCR (ref.[6]) spectra were measured with varied coherence transfer delays mentioned in the following text; the usual delay for ^1H-^{13}C polarization was 12 ms.

Calculations

The assumed molecular structures were studied by semiempirical quantum chemical methods AM1 (ref.[7]) using the GAMESS set of programs[8,9] running on a Silicon Graphics station Indy. The geometries of the reactants, products, reaction intermediates and their complexes with trimethylamine were fully optimized using the gradient optimization routine in the program and all the stationary states were verified by inspecting their Hessian. The calculations were performed in C_1 symmetry.

An initial guess of the transition state (the lowest saddle point connecting reactant and product having a single negative eigenvalue of the force-constant matrix) was obtained from the reactant and product geometries using the algorithm developed by Dewar et al.[10] and it was further optimized by the quadratic approximation method of GAMESS. Then, the intrinsic reaction coordinate (IRC) was calculated to verify whether the obtained transition state really connects the original reactant and product.

RESULTS AND DISCUSSION

The numbering of carbon and oxygen atoms used in the following discussion is shown for the reactants 3-nitrophthalic anhydride (**2**) and 2-hydroxyethyl methacrylate (**1**) in Scheme 1. Numbering of the possible reaction products with the ester group in ortho or meta position to the nitro group (**3** and **4**, respectively), is analogous, oxygen 2 of the anhydride goes into the non-esterified carboxyl. The numbering of the protons is the same as that of the attached carbons in all structures considered.

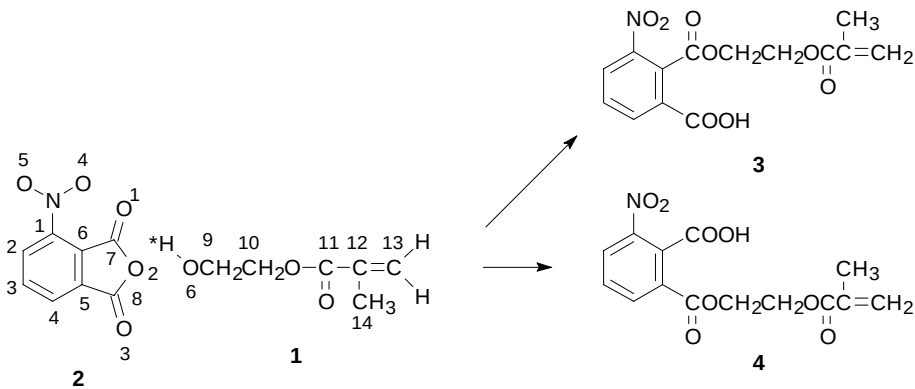

SCHEME 1

Identification of the Isomers and Proof of Their Structure

Figure 1 shows the ^{1}H and ^{13}C NMR spectra of the crude reaction mixture of both reaction products. The signals of the aliphatic part can be easily assigned by comparison with other **1** esters and using COSY spectrum. As for the aromatic protons, the relevant part of the COSY spectrum shown in Fig. 2 reveals that protons 2 and 4 of one of the isomers happen to be magnetically equivalent and form thus a doublet by coupling with proton 3 which, accordingly, gives a triplet. In the other isomer, protons 2 and 4 have slightly shifted signals and form thus a multiplet with essentially a triplet structure whereas proton 3 gives again a slightly distorted triplet signal. By integration of the signals, the molar ratio of the two signals can be determined to be almost exactly 3 : 1.

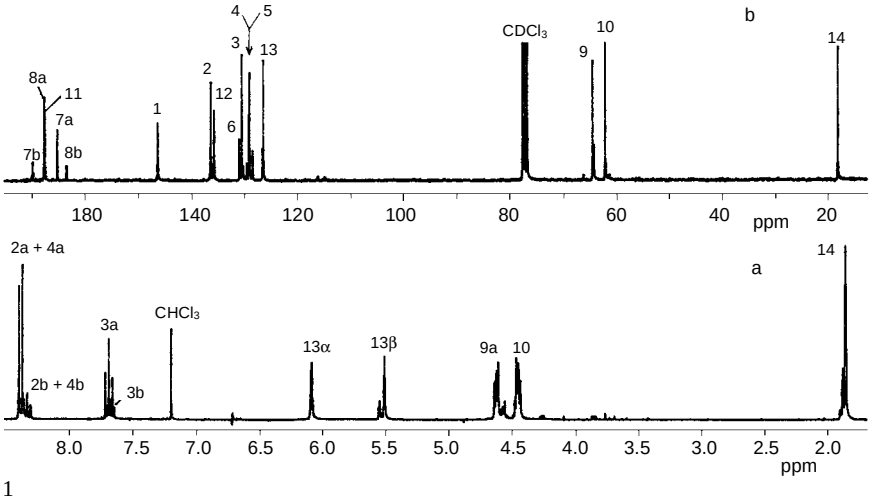

FIG. 1

^{1}H NMR (a) and ^{13}C NMR (b) spectra of the products of the reaction of **1** with **2**

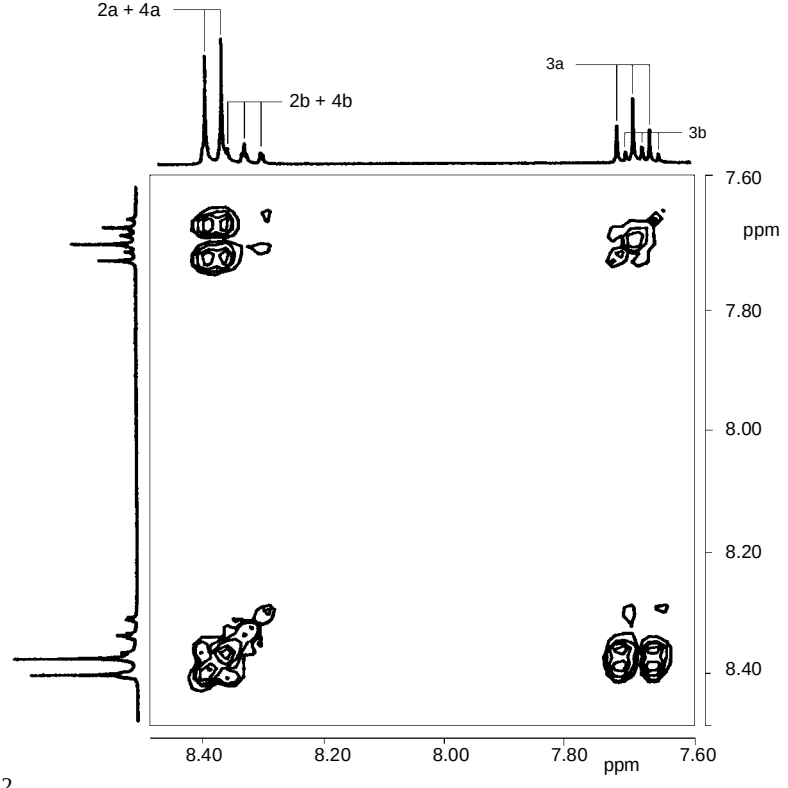

FIG. 2

Aromatic part of the ^{1}H COSY spectrum of the products of the reaction of **1** with **2**

An obvious method for the assignment of the signals to the isomer **3** or **4** is the NOESY or, alternatively, ROESY spectrum considering the principially possible transient vicinity of protons 4 and 9 in **4**. However, neither of these methods gave conclusive results even if their mixing times were varied in the range 0.5 to 1.2 s. Evidently, the more populated isomer with sufficiently sharp signal of proton 2 is either identical with **3** or avoids the conformations in which protons 4 and 9 are close enough to give a conclusive NOE. The problem must thus be solved using ^{13}C NMR.

Relevant parts of the ^{13}C basic, INEPT and APT spectra of **3** and **4** mixture are given in Fig. 3. Figures 4 and 5 show direct and long-range ^{1}H-^{13}C correlations obtained by HETCOR and COLOC, respectively. Due to the fact of the magnetic equivalence of protons 2 and 4 and the tight bonding in the aromatic ring, the 2 + 4 proton signal correlates in COLOC with carbons 2, 4, 5, 6, and 8 when the ^{1}H-^{13}C polarization delay is 20 ms. With the same delay, proton 3 correlates with carbons 1, 3 and 5. The missing correlations in the aromatic ring can be obtained by 1D SSLR INEPT by variation of the polarization transfer delay from 16 to 30 ms. The most interesting feature of the COLOC spectrum is a rather unusual polarization transfer from proton 9 to carbon 7, i.e. along the H–C–O–C bonding. Such type of unexpected polarization transfer has been observed by us in several different structures[11]. In the present case, the incident

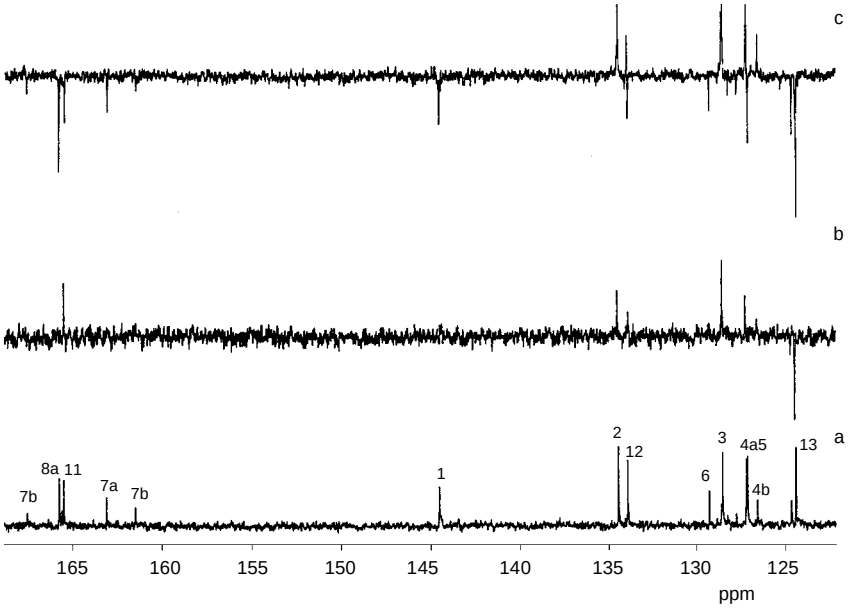

FIG. 3
Relevant parts of the a conventional, b INEPT and c APT ^{13}C NMR spectra of the products of the reaction of **1** with **2**

cross-peak in the COLOC spectrum is certainly not an artefact and the corresponding polarization transfer can be alternatively demonstrated by the SSLR INEPT technique.

The polarization transfer just said identifies the ester carbonyl signal of the predominant isomer. It is now possible to use several different techniques to prove that this carbonyl is in the ortho position to the nitro group. In our experience[12], 1D superselective long-range-relayed polarization transfer (SSLR HCCR) is often superior to analogous 2D techniques because of its sensitivity. In this method, polarization is transferred from a selected proton to a more or less vicinal carbon, according to the transfer evolution delay chosen. The carbon coherence is then relayed to another carbon which, again, is chosen by the duration of the second evolution delay. Finally, double quantum filtration is used to suppress other than the relayed coherences. Due to the low incidence of two ^{13}C nuclei in their natural abundance and the corresponding low intensity of the relayed signal, the suppression is always only relative and other but easily identified signals appear in the spectra. Also, due to the sine time dependence of the antiphase coherences and to the similarity of the two- and three-bond C–C couplings,

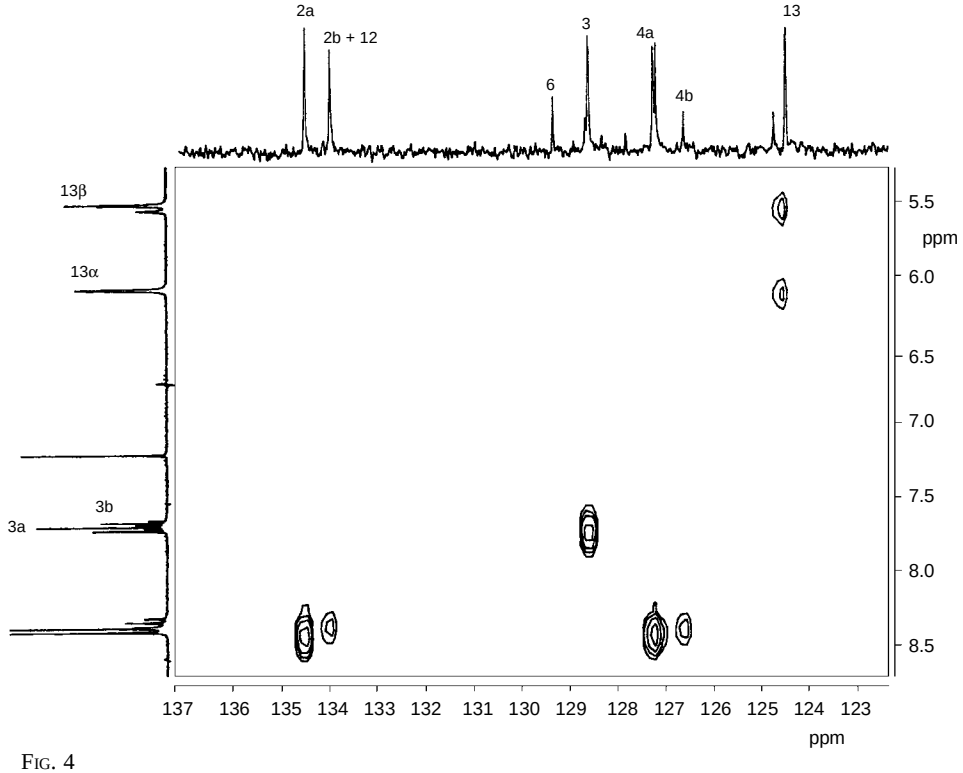

FIG. 4
Relevant part of the ^{1}H-^{13}C HETCOR spectrum of the products of reaction of **1** with **2**

especially in the aromatic ring, the coherence is usually relayed to more than one carbon nucleus. More than one SSLR HCCR spectrum must thus be measured to get a clear picture of the bonding situation.

Figure 6 compares the relevant part of the conventional ^{13}C NMR spectrum with SSLR HCCR spectra with the selective excitation of protons 3 (b,c) and 9 (d) of the predominant isomer. In all relay spectra, a 20 ms C–C coherence transfer evolution period was used, i.e., transfer to all near-neighbour carbons was allowed. If the primary polarization transfer (PPT) from proton 3 is targeted to the directly bonded carbon (d_2 4 ms), we get (cf. Fig. 6b) signals of carbons 3 (rest after Q2 filtration), 2, 4 and 1, 8 (weak). If the target of PT is the next-to-one carbon (d_2 12 ms), signals 2, 1, 7, 8 mainly occur. If proton 9 is excited (Fig. 6d) and PPT is to carbon 7, signals of carbons 7, 6 and 1 are prominent in the spectrum. If PPT is to carbon 1 (d_2 25 ms), signals of carbons 1, 6, 4, 3, and even 2 are seen in the spectrum (Fig. 6e) besides the carbon 11 and 12 signals of the alcoholic part of the molecule. From these results, one can decide

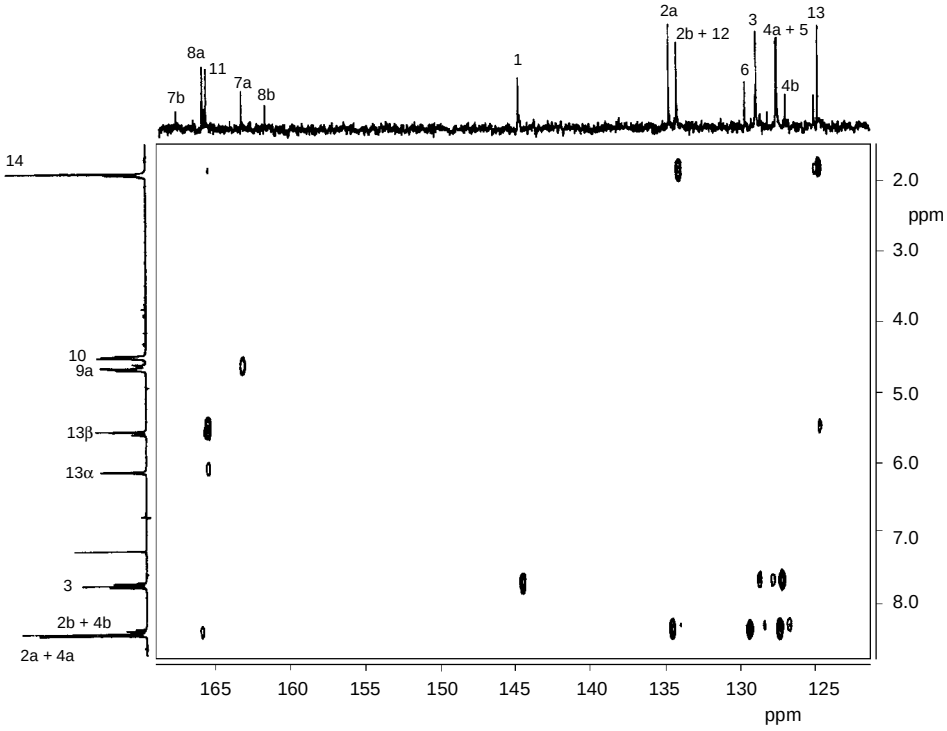

FIG. 5

Relevant part of the long-range ^{1}H-^{13}C HETCOR (COLOC) spectrum of the reaction of **1** with **2** (d2 = 20 ms, d3 = 30 ms)

that the carbonyl of the main ester group is 7, i.e. the neighbour of 6 and 1. In other words, the prominent ester group is in ortho position to the nitro group. The more populated product is thus **3**.

Theoretical Explanation of the Reaction Course

The following calculations were done using the semiempirical quantum chemical SCF method AM1. Instead of **1**, methanol was considered to be the reaction partner in esterification to avoid calculating pitfalls associated with too many degrees of freedom. As it will be clear from the following discussion, the decisive interactions in the reaction mechanism are those of the $HOCH_2$ group with **2**, the rest of the **1** molecule providing only minor contribution. We also start the discussion with the **2**–MeOH interaction although the real experiment was done under triethylamine catalysis. Again, the reason is partly that of methodology (avoiding unimportant local energy minima) and partly heuristic (explaining the core driving forces of the relative regioselectivity).

In Table I, net charges of selected atoms calculated for the optimized **2** structure are given, in Table II the corresponding bond orders. In all the following discussion, O6 means the oxygen atom in methanol. As one can see, there is no unequivocal clue to the

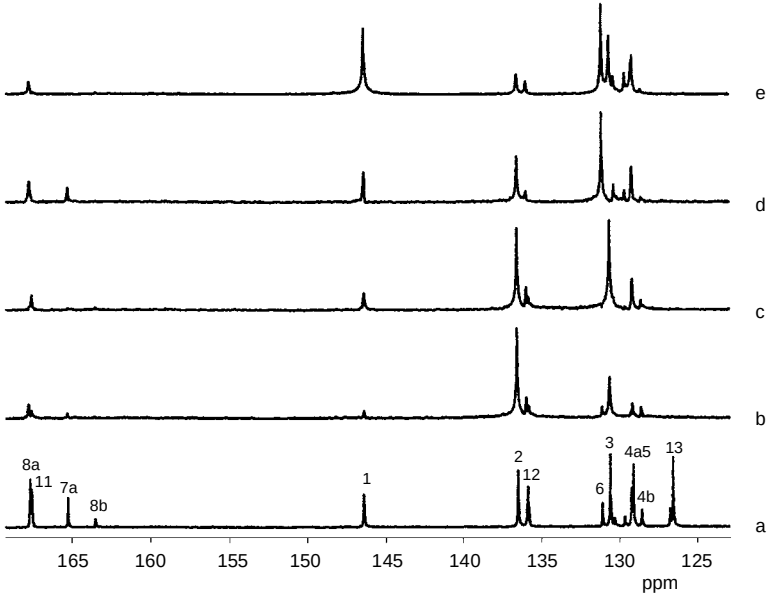

FIG. 6
Relevant part of the ^{13}C NMR spectrum (a) compared with SSLR HCCR spectra. Primary excitation of proton: b, c H3, d, e H9. Value of d_2: b 4 ms, c, d 12 ms, e 25 ms

regioselectivity of the reaction with alcohol in this structure as such: on the one hand, the order of the C7–O2 bond is slightly lower than that of C8–O2, on the other C7 has a slightly lower positive net charge and is thus somewhat less prone to nucleophilic attack than C8.

When searching through the energy hypersurface of the possible approaching of the **2** and MeOH molecules, we identified several intermediate hydrogen-bonded complexes from which two lowest in energy can be considered the immediate precursors of the corresponding transition states of the two possible courses of MeOH reaction with **2**. As is often the case with polar molecules, the intermediate complexes are lower in energy than the non-interacting molecules so that they could wrongly be considered an obstacle rather than a passage to the transition state. However, the same interactions which stabilize these intermediate complexes usually lower the energy of the corresponding transitions states, too. Following the Eyring principle of the lowest energy reaction path (which is surely an approximation but a rather sound one to the actual manifold of reaction trajectories), we must thus consider these intermediate complexes first.

The structures of the respective intermediate complexes **3*** and **4*** are shown in Figs 7a, 7b, their net charges and bond orders are again in Tables I and II. In Figs 7a, 7b as in all the following, the molecular geometries are shown in most perspicuous projec-

TABLE I
AM1 net charges in **2**, intermediate complexes **3***, **4*** and transition states $\mathbf{3}^+$, $\mathbf{4}^+$

Atom	**2**	**3***	**4***	$\mathbf{3}^+$	$\mathbf{4}^+$
C1	–0.07	–0.04	–0.05	–0.08	–0.08
C5	–0.14	–0.16	–0.14	–0.11	–0.15
C6	–0.07	–0.04	–0.07	–0.08	–0.05
C7	0.34	0.42	0.41	0.50	0.45
C8	0.35	0.41	0.42	0.44	0.48
C9	–0.07	–0.19	–0.19	–0.24	–0.24
O1	–0.16	–0.20	–0.19	–0.19	–0.19
O2	–0.24	–0.24	–0.24	–0.60	–0.62
O3	–0.23	–0.23	–0.24	–0.39	–0.21
O4	–0.35	–0.34	–0.34	–0.37	–0.34
O5	–0.30	–0.31	–0.30	–0.33	–0.32
O6	–0.33	–0.42	–0.41	–0.27	–0.28
H*	0.20	0.26	0.25	0.39	0.40

tions. The both the aromatic and anhydride moyeties are essentially planar but lean out of the plane of the paper to show the rest of the incident system.

Generally, there are only minor differences in both types of structure parameters of these two complexes. There is, however, a stronger cumulative hydrogen bond of H* to

TABLE II
AM1 bond orders in **2**, intermediate complexes **3***, **4*** and transition states $\mathbf{3}^+$, $\mathbf{4}^+$, $\mathbf{3}_\mathbf{a}^+$, $\mathbf{4}_\mathbf{a}^+$

Bond	**2**	**3***	**4***	$\mathbf{3}^+$	$\mathbf{4}^+$	$\mathbf{3}_\mathbf{a}^+$	$\mathbf{4}_\mathbf{a}^+$
C6–C7	0.91	0.91	0.91	0.94	0.80	0.93	0.80
C7–O1	1.94	1.92	1.93	2.00	1.71	1.99	1.69
C5–C8	0.92	0.92	0.92	0.82	0.94	0.82	0.94
C8–O3	1.90	1.90	1.89	1.69	1.99	1.68	1.96
C7–O2	0.94	0.94	0.94	0.12	1.31	0.04	1.33
C8–O2	0.96	0.96	0.95	1.31	0.07	1.31	0.03
O6–C7	–	0.001	–	0.62	–	0.71	–
O6–C8	–	–	0.001	–	0.67	–	0.77
H*–O1	–	0.003	–	0.01	–	0.01	0.006
H*–O4	–	0.003	–	0	0	0	0
H*–O2	–	–	0.002	0.04	0.08	0.12	0.13
H*–O3	–	–	0.001	0.003	0.01	0.008	0.01
H*–N	–	–	–	–	–	0.01	0.05

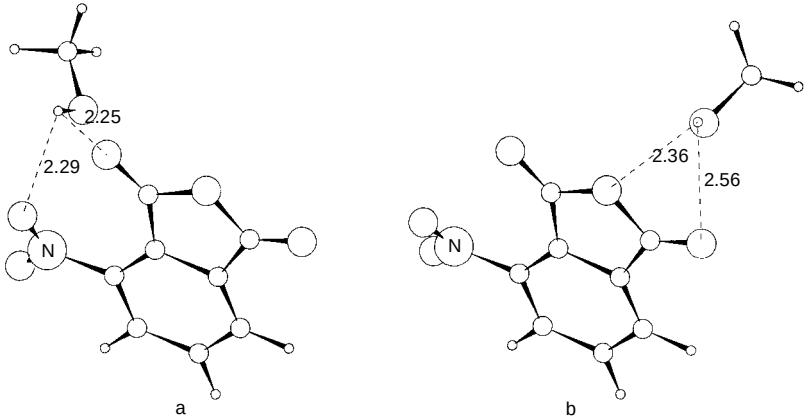

FIG. 7
AM1-optimized intermediate complexes in the reaction of **2** with methanol: a **3***, b **4***

the respective oxygens of **2** (O4 and O1) in **3*** in comparison with those (O3 and O2) in **4***. It is quite possible that this hydrogen bonding is the main interaction which leads to the preference of $\mathbf{3}^*$ though not, as we show below, of the corresponding transition state $\mathbf{3}^+$. The fully optimized transition states $\mathbf{3}^+$ and $\mathbf{4}^+$ obtained by the computational method described above are shown in Figs 8a, 8b, the net charges of their important atoms and the orders of their bonds are again given in Tables I and II, respectively. As one can see, the hydrogen bonds just mentioned have no importance in the transition states as such. This can only be expected because H^* must be transferred and preliminary bonded to O2 in both transition states (which is fully reflected by the corresponding H^*–O2 bond order in Table I). Both C7 (in $\mathbf{3}^+$) and C8 (in $\mathbf{4}^+$) increase further their positive charges in the respective transition states in comparison with the corresponding intermediate complexes. This change is somewhat larger in $\mathbf{3}^+$ and is more than balanced by the increase in the negative charge on O2 (which takes up the proton H^* further down the reaction coordinate) and, interestingly enough, by the increase in bonding to the attached oxygen (O1 in $\mathbf{3}^+$ or O3 in $\mathbf{4}^+$). O6 loses a part of negative charge acquired in the complexes by investing the electron density into the respective fractional bonds, O6–C7 or O6–C8 (cf. the corresponding bond orders in Table II). As one can see, the relative stabilization of the transition states is due to a complex interplay of electron densities in the vicinity of the reaction site.

It should be borne in mind, however, that neither net charges, nor bond orders are observables and must thus be considered with some caution, especially in the case of semiempirical calculations. Energy, on the other hand, is an observable quantity and one of the quantities to which the parameters of semiempirical methods are fitted. Figure 9 shows the energy diagram for the whole reaction of 1 with MeOH. The relative stabilization of **3*** in comparison with **4*** is predicted to be 7.9 kJ/mol, the difference in the respective activation energies is 12.8 kJ/mol.

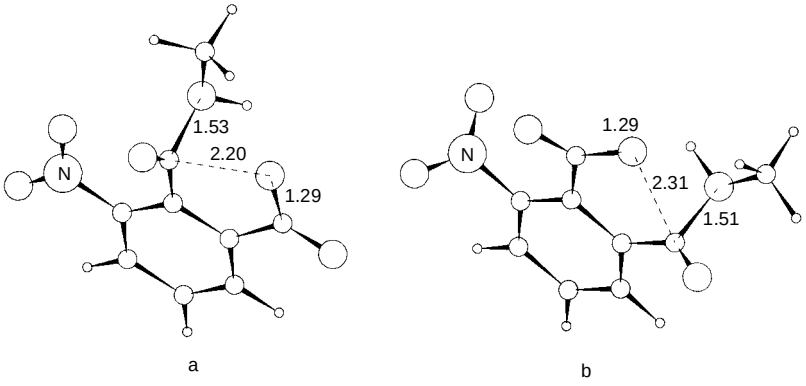

FIG. 8
AM1-optimized transition states in the reaction of **2** with methanol: a $\mathbf{3}^+$, b $\mathbf{4}^+$

The parallel calculations in which trimethylamine was added to reaction system show a very similar picture. The energy diagram for this system is shown in Fig. 10. Here, the relative stabilization of **3*** in comparison with **4*** is predicted to be 5.5 kJ/mol, the difference in the respective activation energies being 14.3 kJ/mol. In comparison with an uncatalyzed reaction, the activation energy is predicted to be lowered by 20.8 and 19.8 kJ/mol, respectively, which appears to be realistic.

The detailed description of the reaction course near the transition state is somewhat different in the case of amine catalysis. Immediately before entering the transition state, H* appears to be weakly bonded to O4, O1 and amine N in the states preceding $\mathbf{3}^+$ and to O3 and N in the $\mathbf{4}^+$ case. In the transition state, the interactions are somewhat changed. The geometry of the respective transition states is shown in Fig. 11, the selected bond orders are given in Table II under the respective headings $\mathbf{3}_\mathbf{a}^+$ and $\mathbf{4}_\mathbf{a}^+$. As one

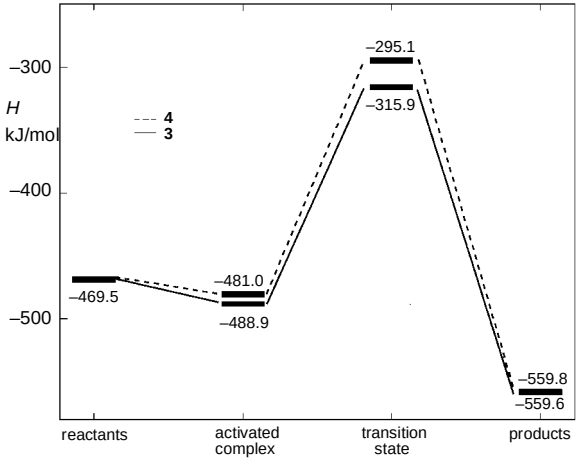

FIG. 9
Energy diagram of the reactions of **2** with methanol; ——— **3**, – – – – **4**. *H* is AM1 heat of formation

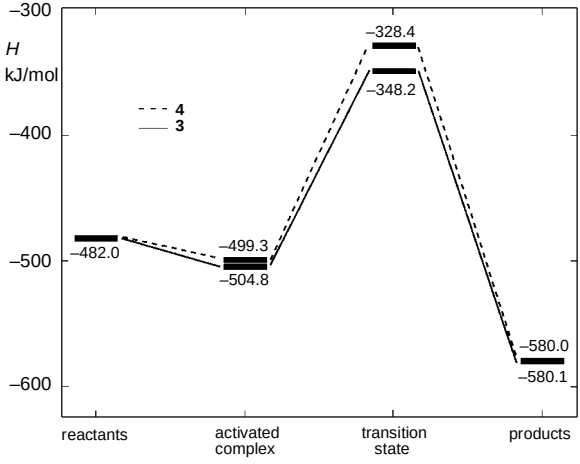

FIG. 10
Energy diagram of the trimethylamine-catalyzed reactions of **2** with methanol; ——— **3**, – – – – **4**. *H* is AM1 heat of formation

can see, most of the bond orders here are very similar to the uncatalyzed case except those directly engaged in bond regrouping: the bonds O6–C7 and H*–O2 are perceptibly stronger and C7–O2 is weaker in $\mathbf{3}_\mathbf{a}^+$ then in $\mathbf{3}^+$ and the same holds for the complementary O6–C8, H*–O2 and C8–O3 when comparing $\mathbf{4}^+$ and $\mathbf{4}_\mathbf{a}^+$. Thus the respective transition states of the catalyzed reaction appear to be somewhat more similar to the reaction products than those of the uncatalyzed case. In both transition states where the amine molecule participates there is perceptible hydrogen bonding between H* and N which is quite consistent with the expected assistence of the catalyst in the proton transfer from the alcohol to the carboxyl. In the case of $\mathbf{4}_\mathbf{a}^+$, this bond is remarkably stronger. The only plausible explanation of this appears to be a somewhat nearer approach of the amine to the rest of the system in $\mathbf{4}_\mathbf{a}^+$ which must stem from slightly lower repulsive interactions between the electron densities around the electronegative atoms. This difference does not result in a higher stabilization of $\mathbf{4}_\mathbf{a}^+$, however.

The predicted energy preferences are in very good agreement with experiment considering the potential of the semiempirical quantum chemical methods. For a system of two fully irreversible reactions exclusively governed by activation enthalpy, the product ratio 3 : 1 corresponds to the 4.6 kJ/mol difference in activation enthalpy at 333 K. Since the products **3** and **4** are almost exactly equal in their energy contents, some equilibration is probable in the course of the reaction. The real activation energy difference of the two reactions can thus be even closer to the predicted one.

CONCLUSION

We have shown that the addition of 2-hydroxyethyl methacrylate to 3-nitrophthalic anhydride preferentially leads to the ester group formed in the ortho position to the nitro group. Quantum chemical calculations using the semiempirical AM1 method cor-

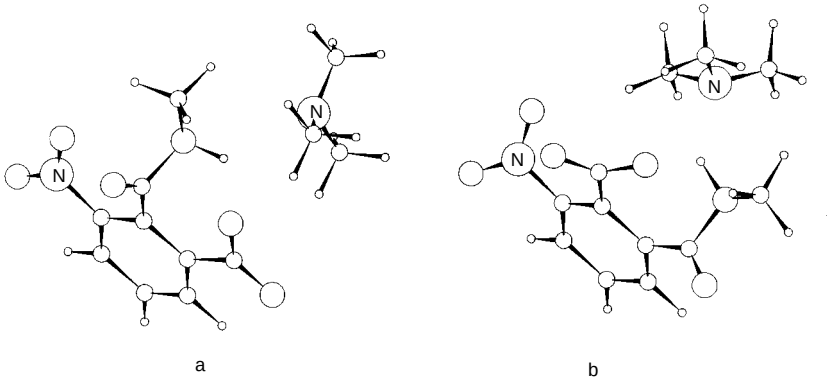

FIG. 11
AM1-optimized transition states in the reaction of **2** with methanol under catalytic assistance of trimethyl amine: a $\mathbf{3}_\mathbf{a}^+$, b $\mathbf{4}_\mathbf{a}^+$

rectly predict the relative regioselectivity of the reaction of methanol with 3-nitrophthalic anhydride, both uncatalyzed and base-catalyzed. By the analysis of the calculation, the reason for the relative preference for one of the products is a subtle interplay of preferential hydrogen bonding and electron density redistribution which cannot be reduced to a simple rule.

The authors thank the Grant Agency of the Czech Republic and the Grant Agency of the Academy of Sciences of the Czech Republic for the financial support under Grants Nos 203/94/0824 and 12/96/K, respectively.

REFERENCES

1. Nagayama K., Kumar A., Wüthrich K., Ernst R. R.: J. Magn. Reson. *40*, 3219 (1980).
2. Bodenhausen G., Kogler H., Ernst R. R.: J. Magn. Reson. *58*, 370 (1984).
3. Bax A., Davis D. G.: J. Magn. Reson. *63*, 207 (1985).
4. Bax A., Morris G.: J. Magn. Reson. *42*, 501 (1981).
5. Kessler H., Griesinger C., Zarbock J., Loosli H. R.: J. Magn. Reson. *57*, 331 (1984).
6. Kriz J., Masar B., Vlcek P.: Makromol. Chem. *194*, 1435 (1993).
7. Dewar M. J. S., Zoebisch E. G., Healy E. F., Stewart J. J. P.: J. Am. Chem. Soc. *107*, 3902 (1985).
8. Dupuis M., Spangler D., Wendolski J. J.: *Program QG01.NRCC Software Catalog 1980*, p. 1. University of California, Berkeley 1980.
9. Schmidt M. W., Baldridge K. K., Boatz J. A., Elbert S. T., Gordon M. S., Jensen J. J., Koseki S., Matsunaga N., Nguyen K. A., Su S., Windus T. L., Dupuis M., Montgomery J. A.: J. Comput. Chem. *14*, 1347 (1993).
10. Dewar M. J. S., Healy E. F., Stewart J. J. P.: J. Chem. Soc., Faraday Trans. 2 *80*, 227 (1984).
11. Kriz J.: Unpublished results.
12. Kriz J., Dybal J., Janata M., Vlcek P.: Magn. Reson. Chem. *32*, S8 (1994).